ATOMISTIC MODELING OF CARBON CO-IMPLANTS AND RAPID THERMAL ANNEALS IN SILICON

Nikolas Zographos[1], Ignacio Martin-Bragado[2]

[1]Synopsys Switzerland LLC, Affolternstrasse 52, 8050 Zürich, Switzerland
[2]Synopsys, Inc., 700 East Middlefield Road, Mountain View, California 94043, USA

ABSTRACT

Carbon co-implantation after pre-amorphization implantation is a promising candidate for ultra shallow junction formation for advanced CMOS technologies due to its ability to suppress transient enhanced diffusion of dopants in silicon. Modeling the interaction of carbon with point defects is important for the development of these techniques. In this paper, we demonstrate a comprehensive atomistic model for carbon implantation, diffusion, clustering, and interaction with End-Of-Range (EOR) defects.

INTRODUCTION

In deep-submicron MOSFET devices, ultra shallow junctions with low sheet resistance are required to achieve good device performance. To fulfill the ITRS [1] requirements for the 45nm technology, conventional combinations of an implantation and rapid thermal annealing are not adequate anymore and new approaches are required. Carbon co-implantation after pre-amorphization implantation has been reported [2] to reduce the junction depth due to the suppression of transient enhanced diffusion and is widely studied for process integration.

According to the ITRS [1], the potential reduction of technology development costs by appropriately used TCAD is at 40%, demanding, amongst others, comprehensive atomistic modeling to complement experiments and continuum models. Continuum models for ultra shallow junction formation with carbon co-implantation have been reported so far [2][3]. In this work, we use an atomistic modeling approach that accounts for carbon diffusion by the kick-out mechanism, the Frank-Turnbull mechanism, and carbon clustering with silicon interstitials. In addition, we include the interaction of carbon with End-Of-Range (EOR) defects. We show that, integrated in a kinetic Monte Carlo (KMC) process simulator [4], these models can accurately simulate carbon marker layer and co-implant experiments with rapid thermal anneals (RTA).

MODEL

The influence of carbon on the diffusion of dopants in silicon is due to changed concentrations of the intrinsic point defects in carbon-rich regions. Substitutional carbon is known [5] to suppress the diffusion of boron and phosphorus while it enhances the diffusion of arsenic and antimony. On one hand, immobile substitutional carbon atoms transform into interstitial carbon through a kick-out reaction with silicon self-interstitials ($C + I \leftrightarrow C_i$) [5]. In addition, carbon can dissociate in a carbon interstitial pair and a vacancy by the Frank-Turnbull reaction ($C \leftrightarrow C_i + V$) [5]. The highly mobile interstitial carbon tends to diffuse out of carbon-rich regions, leading to an under-saturation of self-interstitials and a super-saturation of vacancies in these regions. On the other hand, the clustering of carbon atoms at high concentrations can trap excess interstitials leading to a further suppression of the self-interstitials density.

The KMC process simulator [4] covers atomistic simulation of ion implantation, diffusion, and activation. The cascades and damage accumulation of the implanted ions are simulated by a fully integrated binary collision approximation campaigned by simulation of dynamic annealing. Amorphization of the crystalline silicon substrate by ion bombardment as well as solid phase epitaxial re-growth (SEPR) during subsequent annealing is included in the simulation. Migration of point defects and dopant defect pairs, including different charge states and Fermi-level effect, as well

1-4244-1227-7/07/$25.00

as the clustering of point defects and dopants is also modeled. KMC accounts for the whole extended defect evolution, that is the nucleation, growth, and dissolution of the initial small irregular clusters, the {311} defects, and the dislocation loops [6]. Boron diffusion in crystalline silicon is described by boron-interstitial and boron-vacancy pair migration, and boron activation/deactivation by boron-interstitial complexes B_mI_n. In addition, direct boron diffusion in amorphous silicon [7], temperature dependent boron activation [8] and B_2 cluster incorporation [9] during SPER are simulated. A three phase segregation model with impurity trapping at the Si/SiO_2 interface governs the dopant dose loss.

In this framework, we allow carbon diffusion by the kick-out mechanism and the Frank-Turnbull mechanism. Substitutional carbon and carbon interstitial pairs are assumed to be electrically neutral. The carbon clustering with silicon interstitials forming clusters C_mI_n of various sizes is following the model of Pinacho [10], which got extended by more interstitial rich cluster configurations. The C_mI_n clusters can trap and emit carbon interstitial pairs as well as interstitials and vacancies. To explain the carbon segregation at EOR defects, the model assumes that the carbon interstitial pairs are broken up at the edges of the extended defects and the interstitial is trapped by the extended defects. We assume carbon to be immobile in amorphous silicon for lack of better knowledge, and a temperature dependence of the fraction of carbon to be incorporated as substitutional or clustered in C_2 during SPER.

RESULTS AND DISCUSSIONS

A given macroscopic diffusivity for carbon ($6.11 \exp(-3.293\text{eV}/kT)$ cm^2/s [11]) implies a fixed relation of carbon interstitial binding and migration energy according to Martin-Bragado [12]. We assume a binding energy of 1.5eV as suggested by [10], leading to the migration energy of 0.791eV. Marker layer experiments [10][13][14] were used for the verification of these parameters as well as for the calibration of the cluster potential energies. Figs 1 and 2 show a good agreement of the carbon profiles.

In addition, the retarded diffusion of boron marker layers in the carbon rich region shows the interstitial absorption by the presence of carbon, as depicted in Fig 1. Preparatory, we have calibrated the boron independently of carbon for a wide range of marker layer and ultra shallow junction experiments.

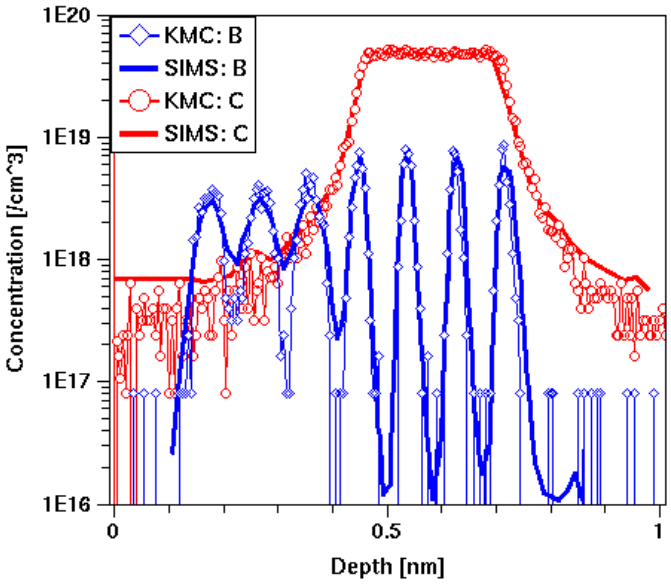

Figure 1: Diffusion of B and C marker layers (900°C, 45min) [13]. Retarded B diffusion due to interstitial under-saturation in carbon-rich regions is observed.

Fig 2 shows the comparison of our model the experimental data obtained by Laveant [14]. Larger carbon interstitial clusters are used to match the carbon profile of higher concentration. In addition, a Frank-Turnbull like mechanism for carbon interstitial clusters to emit vacancies (C_mI_n <-> C_mI_{n+1} + V) was included to predict the enhancement of the vacancy-mediated diffusion of antimony.

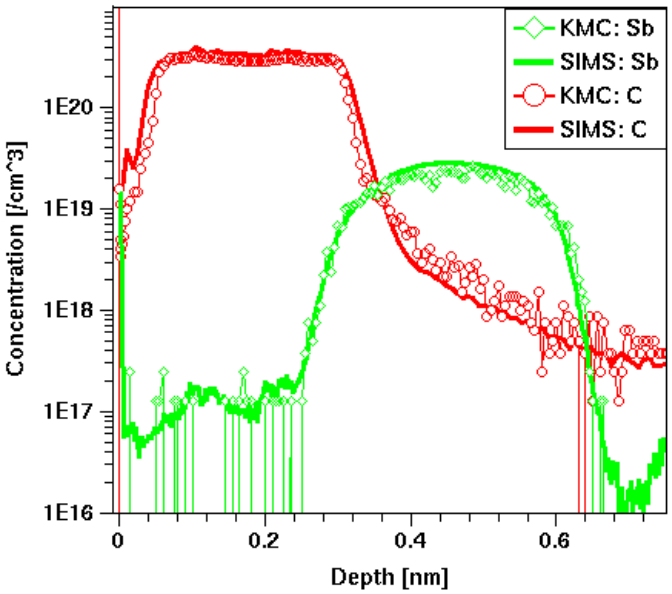

Figure 2: Diffusion of Sb and C marker layers (900°C, 180min) [14]. Enhanced Sb diffusion due to vacancy super-saturation in carbon-rich regions is observed.

Finally, the cocktail implant plus spike RTA experiments of Moroz [2] for *p*-type source and drain extensions can be accurately predicted with our model (Figs 3 and 4). Germanium is only modeled for the pre-amorphization implantation of $1x10^{15}cm^{-2}$ at 20keV to generate an amorphous layer of 36nm, but any chemical or stress effects due to germanium are discarded. To match the annealed carbon profiles, which shows carbon segregation in the EOR region, we allowed the interaction of mobile carbon interstitial pairs with extended defects. While the interstitials are attached to the extended defects, the carbon accumulates in the EOR region, and eventually forms clusters with interstitials in the vicinity of the EOR defects. As a result, the model closely predicts that carbon inhibits the nucleation of EOR loops as reported by Cristiano [15]. Retarded boron diffusion is accurately modeled by the trapping of interstitials by carbon pairs and clusters. Because the interstitial mediated diffusion of boron is dominating the vacancy mediated one, the interstitial under-saturation and vacancy super-saturation due to the presence of carbon results in an overall reduction of boron diffusion. In addition, the BIC model predicts the correct enhancement of the boron solubility due to lower availability of free interstitials to be clustered with boron.

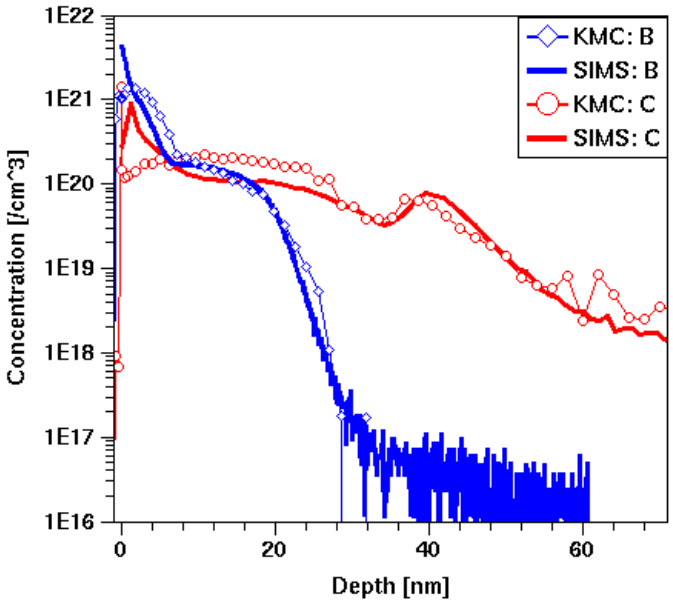

Figure 3: Measured [2] and simulated B and C profiles after Ge pre-amorphization and spike RTA for C $6.5x10^{14}cm^{-2}$ 5keV and B $1x10^{15}cm^{-2}$ 0.5keV implants.

The same models and calibration also give a good agreement with the experimental data of Pawlak [3][16] without germanium pre-amorphization. Fig 5 shows the dependence of the boron diffusion on the implanted carbon dose. Carbon implantation at a dose of $2x10^{15}cm^{-2}$ suppresses boron diffusion to a greater extend because it is slightly amorphizing, and during SPER of the following spike RTA, most of the implanted carbon in the re-crystallized region is placed in substitutional positions, being able to trap interstitials most efficient.

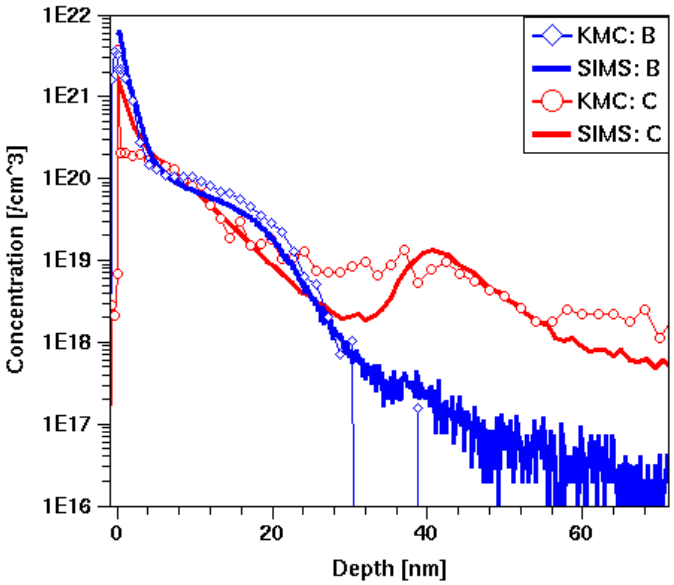

Figure 4: Measured [2] and simulated B and C profiles after Ge pre-amorphization and spike RTA for C $3.3x10^{14}cm^{-2}$ 2keV and B $1x10^{15}cm^{-2}$ 0.2keV implants.

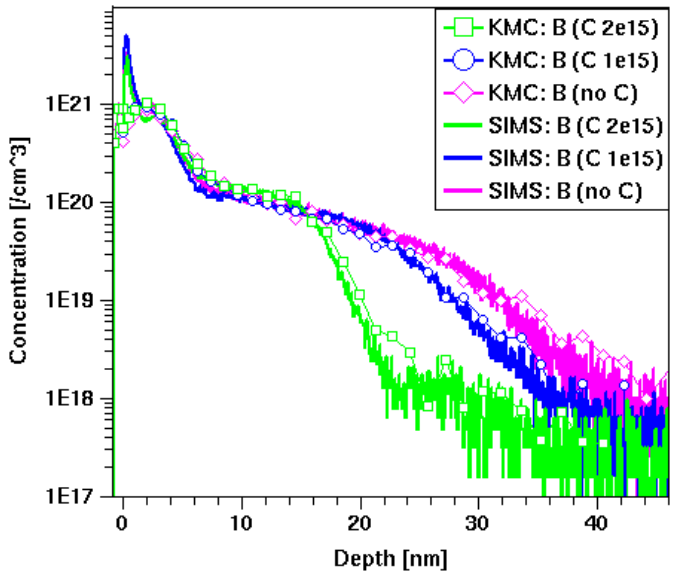

Figure 5: Measured [15] and simulated B profiles after B $7x10^{14}cm^{-2}$ 0.5keV implant and spike RTA for no C co-implant, C $1x10^{15}cm^{-2}$ 6keV co-implant, and C $2x10^{15}cm^{-2}$ 6keV co-implant.

SUMMARY AND CONCLUSIONS

Carbon has appeared in fabrication processes of integrated systems and, consequently, there is a need to model its evolution in silicon. We have formulated an atomistic model for carbon in silicon with an interstitial kick-out mechanism and a dissociative Frank-Turnbull mechanism. For high carbon concentrations, carbon clustering with interstitials inevitably must be considered. We also propose an interaction of carbon with extended defects, which predicts measured carbon accumulation at EOR. This comprehensive model can accurately simulate a wide range of experiments, including carbon co-implantation followed by RTA with and without pre-amorphization, with a single set of calibration parameters.

REFERENCES

[1] ITRS 2006 Update, http://www.itrs.net/reports.html.

[2] V. Moroz, Y.-S. Oh, D. Pramanik, H. Graoui, M. Foad, Appl. Phys. Lett. 87, 051908 (2005)

[3] C. Zecher, D. Matveev, N. Zographos, V. Moroz, B. Pawlak, Mater. Res. Soc. Symp. Proc. 0994-F11-17 (2007)

[4] Sentaurus Process User Manual, Synopsys Inc., March 2007

[5] H. Rücker, B. Heinemann, D. Bolze, D. Knoll, D. Krüger, R. Kurps, H. J. Osten, P. Schley, B. Tillack, and P. Zaumseil, IEDM (1999)

[6] I. Martin-Bragado, I. Avci, N. Zographos, P. Castrillo, M. Jaraiz, ESSDERC (2007)

[7] V.C. Venezia, R. Duffy, L. Pelaz, M.J.P. Hopstaken, G.C.J. Maas, T. Dao, Y. Tamminga, P. Graat, Mater. Sci. Eng. B 124-125, 245-248 (2005)

[8] S. H. Jain, P. B. Griffin, J. D. Plummer, S. Mccoy, J. Gelpey, T. Selinger, D. F. Downey, , J. Appl. Phys. 96, 7357 (2004)

[9] D. De Salvador, G. Bisognin, M. Di Marino, E. Napolitani, A. Carnera, H. Graoui, M. A. Foad, F. Boscherini, S. Mirabella, Appl. Phys. Lett. 89, 241901 (2006)

[10] R. Pinacho, P. Castrillo, M. Jaraiz, I. Martin-Bragado, J. Barbolla, H.-J. Gossmann, G.-H. Gilmer, J.-L. Benton, J. Appl. Phys. 92, 1582 (2002)

[11] P. Pichler, Intrinsic Point Defects, Impurities and Their Diffusion in Silicon, Springer, Vienna 2004

[12] I. Martin-Bragado, P. Castrillo, M. Jaraiz, R. Pinacho, J. E. Rubio, J. Barbolla, Phys. Rev. B 72, 035202 (2005)

[13] H. Rücker, B. Heinemann, W. Ropke, R. Kurps, D. Kruger, Appl. Phys. Lett. 73, 1682 (1998)

[14] P. Laveant, PhD thesis, MPI, Germany 2002

[15] F. Cristiano, C. Bonafos, A. Nejim, S. Lombard, M. Omri, D. Alquier, A. Martinez, S.U. Campisano, P.L.F. Hemment, A. Claverie, Nucl. Instr. Meth. Phys. Res. B 127/128, 22-26 (1997)

[16] B.J. Pawlak, T. Janssens, B. Brijs, W. Vandervorst, S.B. Felch, E.J.H. Collart, N.E.B. Cowern, Appl. Phys. Lett. 89, 062110 (2006)